Volume-phase holographic gratings and their potential for astronomical applications

Samuel C. Barden[a], James A. Arns[b], and Willis S. Colburn[b]

[a]National Optical Astronomy Observatories[*], PO 26732, Tucson, AZ 85726
[b]Kaiser Optical Systems, Inc., PO Box 983, Ann Arbor, MI 48106

ABSTRACT

A diffraction grating technology based upon volume-phase holograms shows promise of enhanced performance for many applications in astronomical spectroscopy over classical surface-relief grating technology. We present a discussion of the underlying physics of a volume-phase grating, give some theoretical performance characteristics, present performance data for a real volume-phase grating, and discuss some potential applications for this grating technology.

Keywords: diffraction gratings, holographic gratings, spectrographs, astronomical instruments

1. INTRODUCTION

In recent years, a new type of grating has been developed using holographic techniques[1]. Rather than being diffracted by surface-relief structures as in a surface grating (generated either by diamond ruling or by a holographic exposure of a photoresist layer), the light undergoes Bragg diffraction as it passes through the volume of a thin layer in which the refractive index is modulated. These volume-phase (VP) holographic gratings show promise for improved performance over classical, low-order, surface-relief gratings in the following areas:

- The "blaze" or efficiency envelope is governed by Bragg diffraction and can be tuned by adjustment of the grating angle for different wavelengths or diffraction orders.
- They can have high diffraction efficiencies approaching 100% for high line density (600 to 6000 l/mm), high dispersion transmission gratings with relatively low dependence on polarization angle.
- The technology can likely produce very large grating sizes (at least 600 by 850 mm).
- Complex grating structures can be produced to minimize optical elements in some spectrograph configurations, simplifying spectrograph design and enhancing spectrograph efficiency.
- The grating is sandwiched between two substrates providing an environmentally stable device which is robust, can be cleaned, can have anti-reflection coatings applied, and is capable of long lifetimes without degradation.
- Grating customization is relatively straightforward as each grating is an original rather than a replica of an expensively ruled master.
- Both transmission and reflection grating geometries are possible.

VP grating technology can improve both the versatility and the efficiency of optical astronomical spectrographs.

A brief overview of the underlying physics is presented and followed by a discussion of both theoretical and actual grating performance. We close with a discussion on many of the various possibilities provided by volume-phase gratings.

2. VOLUME-PHASE GRATING PHYSICS

The diffracting mechanism in VP gratings arises from modulations in the refractive index in the form of fringe planes running parallel to each other through the depth of the grating material and oriented so that the fringes terminate at the surfaces of the volume[2,3]. Figure 1 schematically displays the structure and geometry of four types of VP gratings.

---

[*] Operated by the Association of Universities for Research in Astronomy, Inc. (AURA) under cooperative agreement with the National Science Foundation.

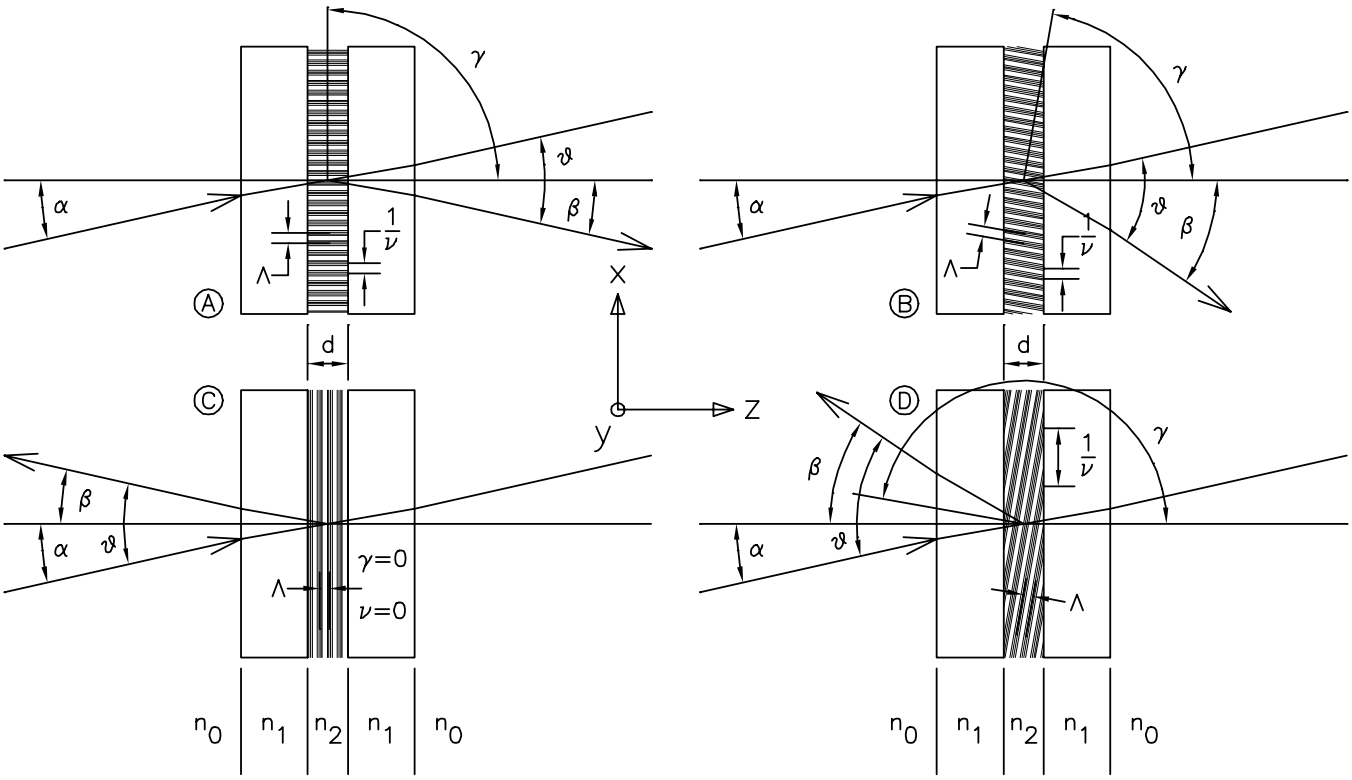

Figure 1. *Some possible VP grating configurations showing Bragg condition diffraction.* ***A****. Transmission grating with fringes perpendicular (*γ *= 90 degrees) to the grating surface (unslanted fringes). In this case the magnitude of* α *equals that of* β *for the Bragg condition.* ***B****. Transmission grating with tilted fringes.* ***C****. Reflection grating with fringes parallel (*γ *= 0) to the grating surface. This grating does not disperse the light since* ν *is zero. Again, the magnitude of* α *and* β *are equivalent for the Bragg condition.* ***D****. Reflection grating with tilted fringes.*

The spacing (1/ν) of the fringe planes as they intersect the surface of a VP grating define the grating dispersion, diffracting light according to the standard grating equation in the same manner as a classical surface-relief grating. The grating equation for a transmissive VP grating can be represented by

$$m\nu\lambda = \sin(\alpha) - \sin(\beta) \tag{1}$$

where *m* is the order of diffraction, ν is the grating frequency, λ is the wavelength of light in free space, α is the angle of incidence in air, and β is the angle of diffraction in air. Light traversing a VP grating, however, is also affected by interaction with the fringes as it travels through the bulk or volume of the grating material. The depth of the grating volume, the intensity or contrast of the fringe structure, and the angular and spectral relationship of the incident light to the Bragg condition determine how much light goes into which order. The Bragg condition for a plane, parallel grating with fringes that are normal to the grating surface (the case shown in Figure 1a) is given by

$$m\lambda = \Lambda\, 2\, n_2 \sin(\alpha_{2B}) \tag{2}$$

where Λ is the fringe spacing of the grating equal to 1/ν for fringe planes orthogonal to the grating surface, and α_{2B} is the Bragg angle in the grating medium. The Bragg condition is met when *m* is an integer and the wavelength and fringe spacing are such that the angles of incidence and diffraction are equal and opposite (with respect to the surface normal). The formulation of the Bragg condition for slanted fringes is slightly more complex, but in that case the angles of incidence and diffraction are symmetric within the grating medium about the fringe planes. Light illuminating the grating at angles significantly outside of the Bragg condition may pass through the grating without being diffracted. However, near the angle at which the Bragg condition is satisfied there is a range of angles for which light will still be efficiently diffracted; these

angles can be thought of as falling within a Bragg envelope and having an angular bandwidth as shown by the sample curve in Figure 2a. Similarly, the wavelength that satisfies the Bragg condition is called the Bragg wavelength, and again there is a Bragg envelope of wavelengths about the Bragg wavelength that are diffracted efficiently as shown in Figure 2b. Wavelengths that are significantly outside the spectral bandwidth may pass through the grating undiffracted. It is this selective aspect which allows these gratings to be tuned for different orders of diffraction and or wavelengths by tilting the grating with respect to the incident beam of light.

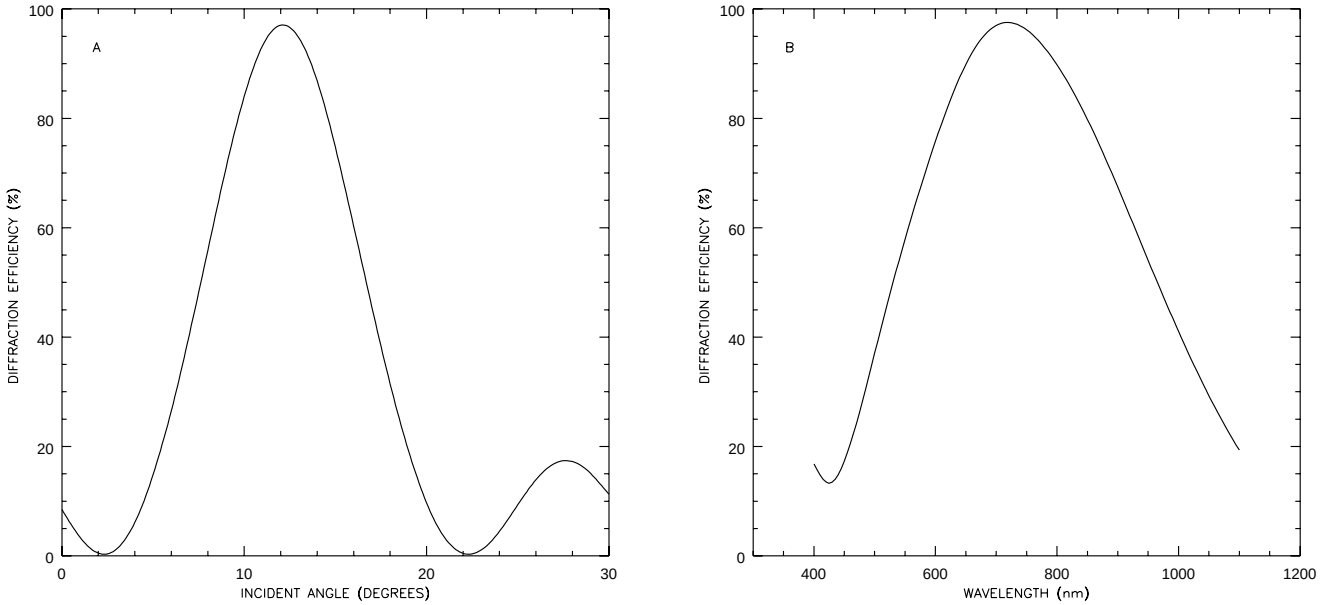

Figure 2. *The angular and wavelength bandwidth Bragg envelopes for a theoretical 600 l/mm grating designed for 1st order operation at 700 nm.* ***A.*** *Angular bandwidth Bragg envelope.* ***B.*** *Wavelength bandwidth Bragg envelope.*

Figure 1 shows the grating parameters (α, β, γ, θ, Λ, d, n_2) which, along with the amplitude of the index of refraction modulation (Δn_2), determine the grating performance. The index of refraction, n_2, for the grating itself is the average value of the modulated refractive index, $n_2(x,z)$, and is approximately represented by

$$n_2(x,z) = n_2 + \Delta n_2 \cos[(2\pi/\Lambda)(x \sin(\gamma) + z \cos(\gamma))] \tag{3}$$

for the case of either slanted or unslanted fringes where Δn_2 is the semi-amplitude of the variation in the index of refraction within the grating volume. The substrate index of refraction is given by n_1 and the refractive index for air is n_0 (assumed to be equal to 1).

Volume-phase gratings can be analyzed by means of either a rigorous coupled-wave analysis[4,5] or a modal analysis[6]; the two approaches are exact and can be shown to be equivalent[7]. In their most rigorous forms, these approaches require computer-derived solutions. Using a simplified coupled-wave analysis that includes only zeroth and first order diffraction, Kogelnik[8] developed a set of closed-form equations that are sufficiently accurate in many cases, and that are widely used in the field of volume holography.

The diffraction efficiency, spectral bandwidth, and angular bandwidth are influenced by the Bragg condition and are functions of the intensity of the grating modulations (Δn_2) and the thickness (d) of the grating volume[4,5,8]. In general, a VP grating with a wide spectral bandpass has a lower peak diffraction efficiency than a grating with a narrower bandpass. For transmission gratings, the peak diffraction efficiency at the Bragg condition is a function of both the grating thickness and modulation intensity. For orthogonal fringe (unslanted) plane gratings the efficiency η at the 1st order Bragg condition is[8]

$$\eta = \sin^2[\pi \Delta n_2 \, d / (\lambda \cos(\alpha_{2B}))] \tag{4}$$

where α_{2B} is the angle within the grating material (where $n = n_2$) given by the relation

$$\sin(\alpha_{2B}) = (n_0 / n_2) \sin(\alpha). \quad (5)$$

The 1st order spectral bandwidth and angular bandwidth for unslanted, transmission gratings are approximated by[8]

$$\Delta\lambda_{FWHM} / \lambda \sim (\Lambda/d)\cot(\alpha_{2B}), \quad (6)$$

$$\Delta\alpha_{FWHM} \sim \Lambda/d \quad (7)$$

where $\Delta\alpha_{FWHM}$ is in radians. The challenge in VP grating fabrication is to produce a grating with appropriate thickness and refractive index modulation to provide the desired peak efficiency and bandwidth performance.

Polarization dependence in VP gratings is dominated by a reduced coupling constant for parallel polarization of light with respect to the plane of incidence (p or TM polarization)[8], whereby Equation (4) becomes

$$\eta = \sin^2\{[\pi \Delta n_2 \, d / (\lambda \cos(\alpha_{2B}))]\cos(\theta_2)\} \quad (8)$$

where θ_2 is the angle within the medium between the incident (α_{2B}) and diffracted (β_2) wavefronts. When the angle between the incident and diffracted waves within the grating equals 90°, the diffraction efficiency for this polarization state goes to zero. Polarization dependencies can be minimized as long as this condition is avoided.

3. GRATING FABRICATION

The VP gratings in this study are fabricated in dichromated gelatin. A thin film of sensitized gelatin is deposited onto a glass substrate and exposed in a holographic exposure system to record an interferometrically produced wave pattern of the desired fringe frequency and orientation. Wet processing transforms the exposed fringes into refractive index modulations within the gelatin. Once the desired grating parameters have been achieved, a cover glass is laminated over the gelatin surface. The substrate may be any glass material; typical optical glasses used are BK7 and fused silica. Anti-reflection coatings can be applied to the substrates to reduce reflection losses. It is also possible to use prisms and plano-convex or plano-concave lenses in the grating assembly.

Contrary to the statement that dichromated gelatin "is not an attractive candidate for high accuracy, because it is difficult to process gelatin in such a way that the modulation pattern is accurately reproduced after a wet-dry processing cycle"[9], this material has been used extensively in holographic components for over twenty five years with a proven record of producing high quality diffraction elements with high diffraction efficiency, high clarity, low scatter, low absorption, and long lifetime when properly treated in the fabrication process and adequately protected against degrading environmental conditions[10,11,12]. Due to the hygroscopic nature of the gelatin, a protective cover glass is required to prevent water vapor from affecting the sensitive film and to protect the grating from contaminants. Properly sealed dichromated gelatin holograms can have lifetimes of at least 20 years if they are given reasonable care and handling. Their application as head-up display components in military aircraft show that elements fabricated in this manner can withstand considerable humidity and temperature extremes.

Figure 3 shows the transmission behavior of dichromated gelatin between 300 and 3000 nm. It is apparent that the material may have a useful spectral range from 300 nm to 2.8 μm. VP gratings are currently and routinely fabricated for use between 400 nm and 1.5 μm. Typical values of n_2, Δn_2, and d obtained with dichromated gelatin gratings are 1.5, 0.02 to 0.10, and 4 to 20 μm, respectively. Line densities (ν) range from 300 to 6000 l/mm.

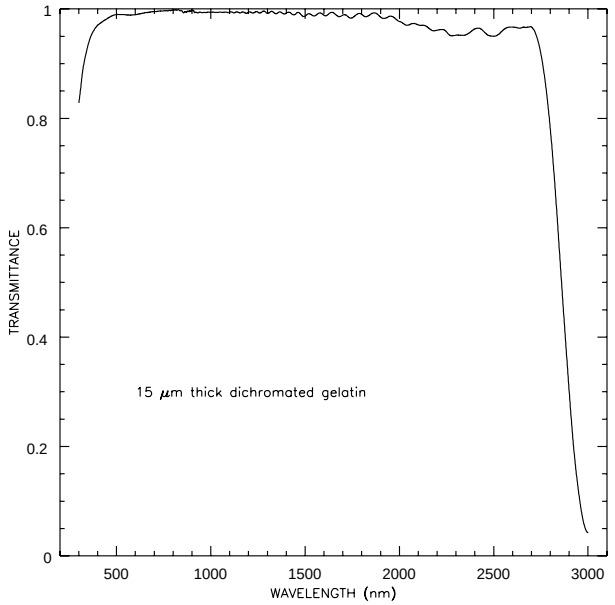

Figure 3. *The transmittance as a function of wavelength for a 15 μm thick layer of uniformly exposed and processed dichromated gelatin.*

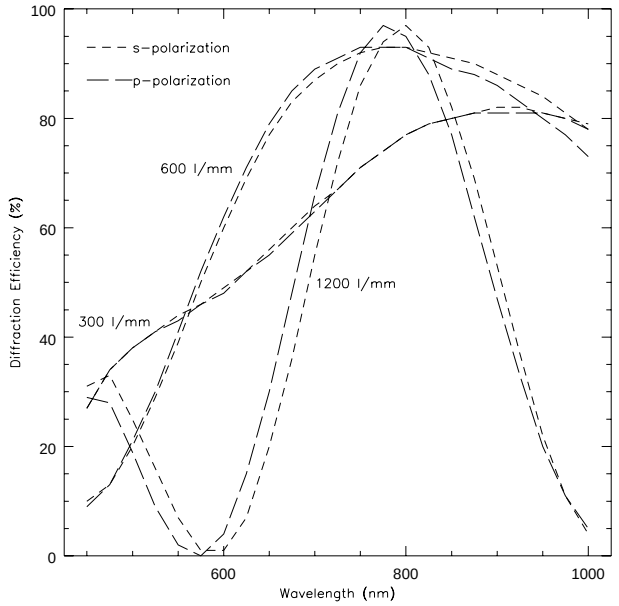

Figure 4. *Rigorous coupled-wave prediction for the diffraction efficiency of three different gratings designed for first order operation at 790 nm. Both s and p polarization states are shown. Material and reflection losses are not included.*

4. GRATING PERFORMANCE

The high diffraction efficiency of dichromated gelatin and the characteristics of Bragg diffraction give the potential for very high efficiency dispersers. Figure 4 shows the theoretically achievable diffraction efficiencies derived through rigorous coupled-wave analysis[4] of three different transmissive VP gratings designed for operation at 790 nm. Notice that the peak diffraction efficiency and bandwidth are traded off against each other. Polarization effects are not very significant. For comparison, a reflective, surface-relief grating blazed at 790 nm will only have a theoretical peak efficiency of about 80% in unpolarized light due to the major dependency of efficiency on the angle of polarization[9].

A 600 l/mm VP grating (HG-700-12) was produced by Kaiser Optical Systems, Inc. (KOSI) for evaluation at the National Optical Astronomy Observatories (NOAO) as part of an effort to design a new technology, high efficiency spectrograph. The grating was designed for optimal efficiency at 700 nm with a bandwidth covering the spectral region spanning 500 to 900 nm in the first order of diffraction. Peak efficiency was specified at 70 to 80% with greater than 50% efficiency at 500 and 900 nm. The grating modulations are perpendicular to the surface of the grating substrate, so the Bragg condition is met when the incident and diffracted angles are the same magnitude.

The absolute efficiency for unpolarized light was measured at NOAO at 400, 500, 633, 700, 800, and 900 nm as a function of incident angle and of diffracted angle. When the grating is illuminated at zero degrees incidence, the majority of the light passes undiffracted into the zeroth order. As the angle of incidence is increased, the level of diffraction increases. Peak diffraction into first order at 700 nm is achieved when the incident angle is about 12 degrees (the first order Bragg condition). At an angle of incidence equal to about 25 degrees, 700 nm meets the Bragg condition for second order diffraction. Figure 5 displays the absolute efficiency of the unpolarized light transmitted and diffracted by the grating at a wavelength of 700 nm as a function of angle of incidence and order of diffraction. A peak efficiency of nearly 80% is achieved for first order diffraction. In comparison with a comparable theoretical VP grating (see Figure 4), this grating is about 10% lower than might be expected. This is attributable to the inclusion of reflective and other material losses in the

measurements of Figure 5 and due to some residual uncertainty in the holographic process which optimizes the grating thickness and the index modulation. Future process refinements will lead to an improved capability of producing gratings with efficiencies that more closely approach the theoretical limits.

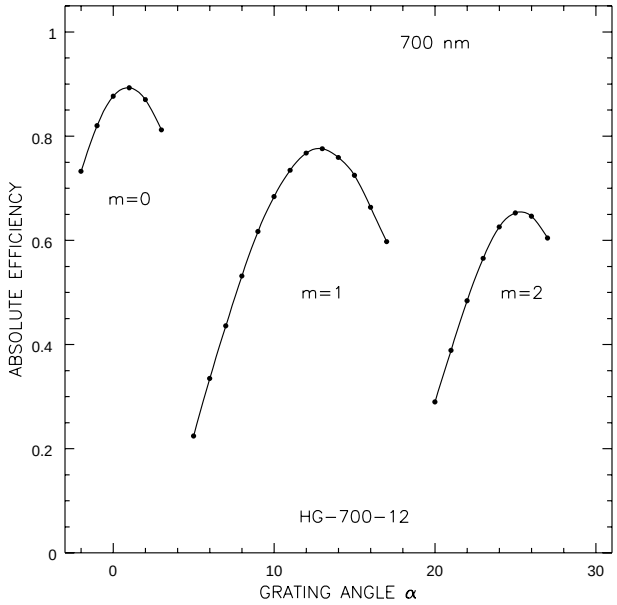

Figure 5. *Absolute efficiency of the 600 l/mm VP grating for unpolarized light as a function of incident angle and diffracted order (m=0,1,2) for 700 nm. Material and reflective losses are included.*

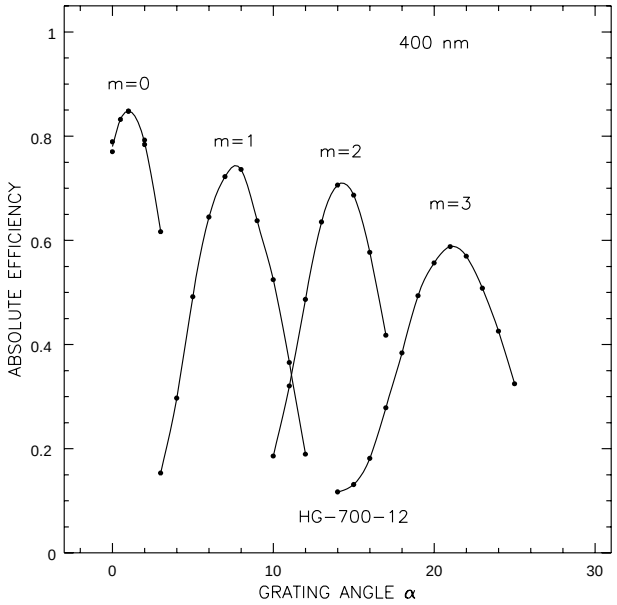

Figure 6. *Absolute efficiency of the 600 l/mm VP grating in unpolarized light at 400 nm for diffraction orders m=0, 1, 2, and 3. Material and reflective losses are included.*

Comparable surface-relief gratings in use at Kitt Peak National Observatory (KPNO) give 70% efficiency at 700 nm in first order (Bausch and Lomb grating 420, 600 l/mm blazed at 750 nm) and 42% for 700 nm in 2nd order (Bausch and Lomb grating 450, 632 l/mm blazed at 1100 nm in 1st order and which has a peak efficiency in 2nd order of 50% at 550 nm). The VP grating shows good performance at the design wavelength in comparison with these other gratings. It also shows superior performance for the 2nd order of diffraction, a region in which it was not specifically designed to function!

At 400 nm, the VP grating still shows excellent performance when aligned for Bragg diffraction at that wavelength for 1st, 2nd, and 3rd order diffraction (7, 14.2, and 21.6 degrees respectively). Figure 6 displays the measured absolute efficiencies for diffraction at 400 nm.

Comparable surface gratings at KPNO are inferior to this grating with only 50% efficiency for 1st order diffraction by a grating originally ruled at KPNO (KPC007, 632 l/mm blazed at 520 nm), 55% efficiency for 2nd order diffraction by another grating ruled at KPNO (KPC22b, 632 l/mm blazed at 850 nm in 1st order), and 40% in 2nd order by a Bausch and Lomb grating (Bausch and Lomb 450, 632 l/mm, blazed at 1100 nm in 1st order). The 3rd order diffraction efficiencies for any of the gratings at KPNO were unavailable for comparison.

The strong performance in higher orders of diffraction for this grating is intriguing and has prompted the authors to further explore the feasibility of high order diffraction VP gratings. Very little research has been conducted in this area since the typical customer for volume holographic devices does not want high order diffraction. As a result, little or no effort has been expended to optimize the performance of a high order VP grating.

The bandwidth of the grating was determined by measuring the efficiency for each wavelength at a specific grating angle, or angle of incidence. Figure 7 shows the equivalent of the "blaze" function as a function of grating tilt for 1st order

diffraction. Tilts of 11 to 12 degrees give the best overall efficiency across the design spectral range of 500 to 900 nm with greater than 55% efficiency and a peak efficiency of nearly 80% between 600 and 700 nm. Note that the grating also makes an excellent, 1st order, blue grating when used at a grating tilt of 8 to 10 degrees. Comparison with the Bausch and Lomb 420 grating (600 l/mm, blazed at 800 nm) at KPNO (Figure 8) shows that the VP grating is about 5 to 10% more efficient across the entire design spectral range.

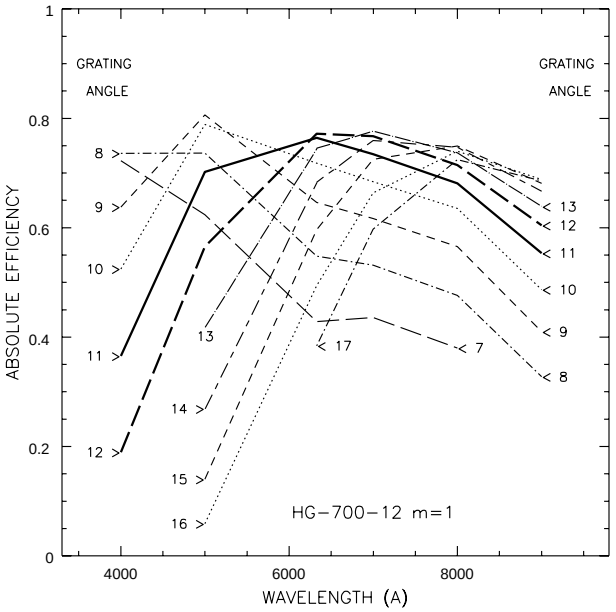

Figure 7. *Efficiency envelope of the 600 l/mm VP grating as a function of incident angle for first order diffraction. Grating tilts of 11 and 12 degrees give the best overall efficiency in the design bandwidth from 500 to 900 nm.*

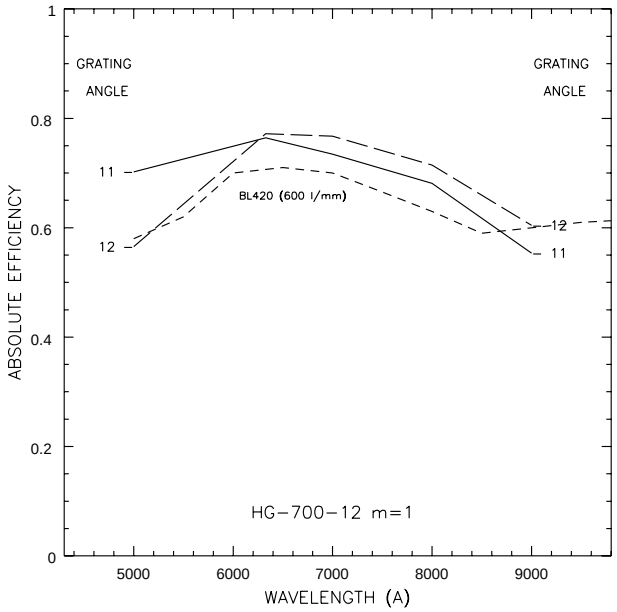

Figure 8. *Comparison of the 600 l/mm VP grating at grating tilts of 11 and 12 degrees to a diamond ruled, 600 l/mm, reflection grating blazed at 800 nm (Bausch and Lomb 420).*

A simple, on-sky test was made with the test VP grating at the KPNO 2.1 meter telescope using a fiber optic feed onto an optical bench. The 22 meter long, 200 μm diameter fiber optic cable fed light from the telescope to a 40 mm diameter achromatic doublet collimating lens. An OG515 high-pass filter was used to filter out 2nd order contamination. A second 40 mm diameter achromatic doublet lens was used to image the light dispersed by the test grating onto a 2048 Tektronix CCD binned 2 by 2 to get 48 μm pixels. The system was first aligned at 12 degrees for first order diffraction from the grating. A standard star was observed and the count rate transformed into a flux rate. The total system (telescope, fiber aperture, fiber, lenses, grating, and detector) efficiency at 670 nm was measured to be 17.0%. The system was then reconfigured to 25 degrees for 2nd order diffraction at the same wavelength and another spectrum obtained. System efficiency was again measured to be 17.2% for 2nd order. Independent determination of the fiber, telescope, aperture, and detector efficiency showed that the two lenses plus grating were 60% efficient in the R band (144 nm bandwidth at 647 nm) in the first order of diffraction. This agrees remarkably well with the laboratory measurements especially given the uncertainty in the atmospheric seeing which was estimated to be variable by about 30% during the course of the observations. Figure 9 displays the spectra for both 1st and 2nd order configurations. Note that the shape of the spectra are dominated by the cutoff filter at 515 nm and by vignetting of the dispersed spectrum by the imaging lens (most notable in the 2nd order spectrum) along with the diminishing quantum efficiency of the CCD detector in the red portion of the spectrum.

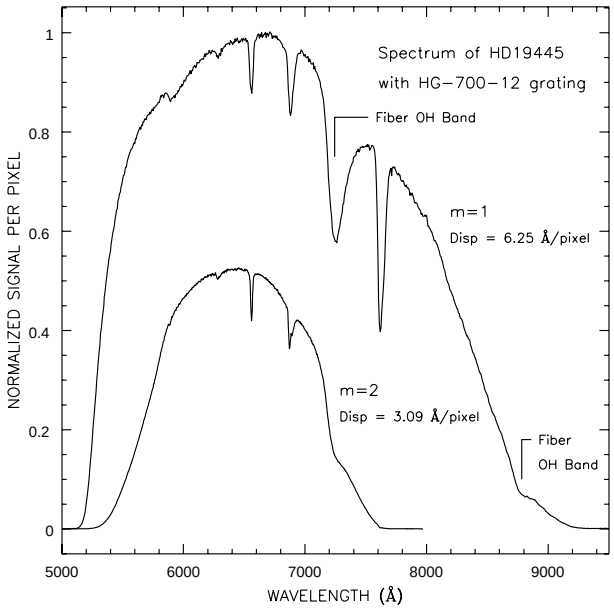

Figure 9. *Stellar spectra obtained in first and second orders of diffraction.. The units of the ordinate axis were selected to remove confusion of the two curves but give the false impression that the 2nd order spectrum has a factor of two lower signal.*

5. POSSIBILITIES

5.1 Transmission gratings

The blazing for surface-relief, transmission gratings, particularly in the red portion of the optical spectrum, can be difficult and sometimes impossible due to the large facet angles and grating depths required. This is particularly true for high dispersion gratings (rulings greater than 600 l/mm for unimmersed gratings)[9]. Inclusion of a prism, making the grating into a grism, allows surface rulings of up to 1200 l/mm before production gets difficult. Many of these restrictions in performance arise from the presence of the surface facets that make the grating. Total internal reflection becomes an issue in the production of such gratings as well as complications in the ability to replicate a surface grating with large and steep grooves.

VP gratings are not limited by either total internal reflection on steep grooves or by the inability to replicate a grating with deep groves since the grating mechanism arises from refractive index modulations rather than surface discontinuities. As such, VP gratings can be fabricated as transmission gratings with line densities of up to and greater than 6000 l/mm. The peak efficiency of a transmission VP grating can also exceed the peak limits of a transmissive surface-relief grating as a consequence of the different diffraction mechanism.

5.2 Reflection gratings

As shown in Figure 1, a reflection VP grating can be produced by creating a sufficient tilt in the holographic fringes with respect to the surfaces of the grating. The peak diffraction efficiency of a reflective VP grating can be quite high but in many cases the bandwidth may be narrower than desired. Some studies have shown that the bandwidth can be increased by modifications in the hologram processing[14,15].

Most reflective VP holographic devices are currently designed to be non-dispersive. There appears to be little activity in the study or production of reflective VP gratings which disperse light into diffraction orders other than zero. Further study of dispersive reflective gratings, however, is warranted and desired. Other than potentially superior performance, the development of large, reflective VP gratings will allow drop-in replacements for many current astronomical spectrographs utilizing reflective surface-relief gratings.

5.3 Grating customization

One of the most frustrating aspects of currently available gratings is the lack of a sufficient sampling in the parameter space of peak efficiency and dispersion, especially with regards to large, astronomical gratings. In order to acquire a grating of desired properties, one must compromise to the closest available catalog grating or have a master grating generated. Quite often, the closest available grating is poorly matched to what is actually desired and large, custom, master, surface-relief gratings are expensive and take a considerable amount of time to generate.

VP holographic gratings are typically not replicas (though there are processes which could replicate VP gratings from a single master[13]) and are relatively straightforward to produce. As such, customization of the grating parameters is more easily attained without a major expenditure in cost or time.

5.4 Complex grating structures

The holographic nature of these gratings allows the stacking of holograms to make a variety of complex grating structures[16,17]. A single grating assembly might contain a second grating with the fringes perpendicular to the first in order to provide cross-dispersion. A second concept is a double grating which disperses light of two different wavelengths into the same angle of diffraction. For example, it would be possible to create a complex grating in which Hα light meets the Bragg condition of the first hologram but not the second and Hβ light satisfies the Bragg condition of the second but not the first VP grating. The correct ratio of line densities in the two gratings would direct both Hα and Hβ into the same angle of diffraction for simultaneous detection by a single detector. A third concept would be a dual grating that divides the light at different wavelengths into different paths to function as a dispersive beam splitter.

5.5 Large gratings

VP gratings are currently fabricated by KOSI and utilized in their line of Raman spectrographs[18]. Although they currently only fabricate gratings of up to 75 by 100 mm in size, their facility can easily accommodate an upgrade for the production of gratings with dimensions of 200 by 280 mm. It is their desire to implement such an upgrade in the very near future. This would allow this interesting and valuable technology to be implemented in astronomical instruments on moderately large telescopes.

With the advent of 8 and 10 meter class telescopes, even gratings of 200 mm in size are becoming too small. The demand is increasing for gratings with sizes of 300 to 400 mm. Classical surface gratings are difficult and expensive to produce due to the wear of the diamond as the grating is ruled. Grating mosaics are possible (e.g. the Echelle grating in HIRES on Keck has 3 gratings to form a 300 by 1200 mm mosaic[19]), but complicated and also costly. State-of-the-art holographic exposure and processing technology is at a level where the production of very large VP gratings could be possible (greater than 600 mm). Indeed, holographically generated surface-relief gratings are already achieving rather large dimensions.

5.6 Wavelength regime

KOSI currently fabricates gratings used in the visible and has recently started producing gratings for use at 1.5 μm. There has not yet been any effort to produce a VP diffraction grating further towards the infrared. Future efforts may attempt to exploit the transmittance of dichromated gelatin out to 2.8 μm. Behavior of dichromated gelatin at cryogenic temperatures would also need some study.

5.7 Line density and diffraction angle

Gratings are currently fabricated with line densities between 300 and 6000 l/mm. Gratings with diffraction angles of up to 72 degrees have been produced at KOSI. Such high diffraction angle gratings are typically immersed to minimize reflection losses on the air-to-glass substrate surfaces.

5.8 Immersed gratings

Immersion of a classical surface grating is another approach for achieving high resolution with a relatively small grating[20] but is difficult due to the fragile nature of the ruled surface. VP gratings, by their nature, are easily immersed.

5.9 High order diffraction gratings

Little study has been expended on the performance of VP gratings at diffraction orders other than zeroth or first. What has been published[21,22,23] and the behavior of the NOAO test grating suggest that it may be possible to fabricate a relatively high order diffraction VP grating. An Echelle-like VP grating could possibly provide greater dispersing power over classical Echelles, especially given the simplicity of immersing a VP grating. Limitations for very high order gratings ($m>3$) may, however, arise from the inability of current holographic materials to achieve the required refractive index modulation for efficient diffraction into those high orders. Further theoretical and empirical study is needed.

5.10 Aberration correction gratings

Non-dispersive, VP holograms are currently used in military head-up display combiners that incorporate aberration correction within the hologram itself. Similar aberration correction can likely be incorporated into VP holographic gratings[24] in a similar fashion to current, concave, holographic, surface-relief gratings.

5.11 Tunable spectrographs

The nature of the test VP grating raises the possibility that a single grating can have a range of performance characteristics depending on the configuration of the spectrograph in which it is used. Such versatility from a single grating is not available with surface-relief gratings. With VP grating technology, it is possible to think of a spectrograph in which the peak efficiency and dispersive power can be tuned to the desired wavelength of interest with a simple change in both the grating angle and the angle between the collimator and the camera (see Figure 10). Although some complexity is added to the spectrograph housing, the need for separate gratings is eliminated or minimized. A simple, fiber-fed, bench-mounted spectrograph could easily accommodate these adjustments, making the instrument much more versatile than a spectrograph with a classical surface grating.

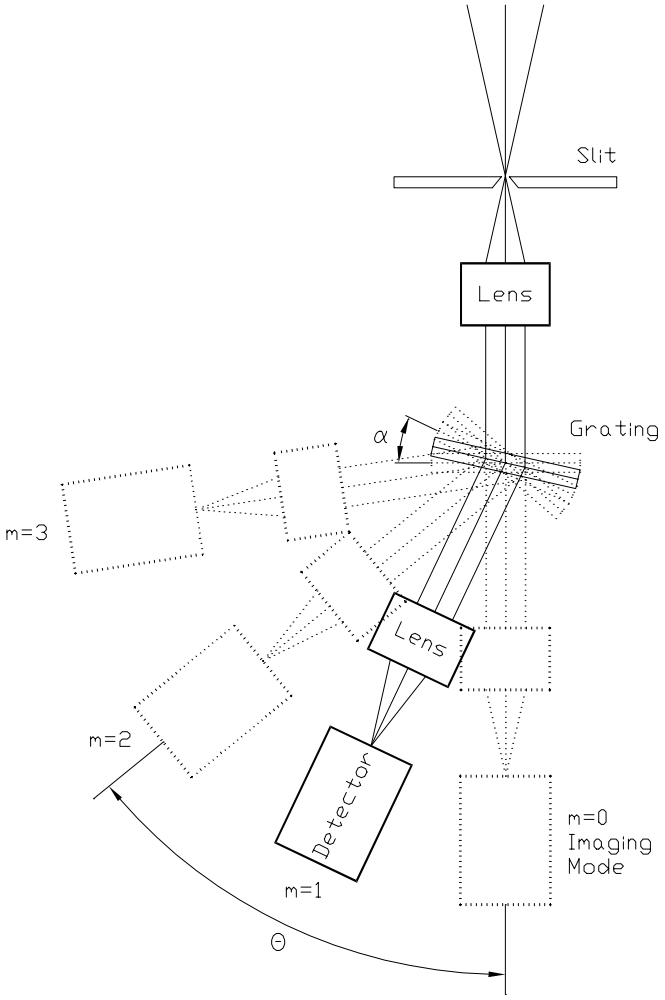

Figure 10. *Schematic of a tunable spectrograph concept in which the camera axis angle (θ) and grating angle (α) are allowed to tilt in order to change the order of diffraction or to peak up the efficiency of the desired wavelength.*

6. CONCLUSIONS

Volume-phase holographic gratings diffract light through a mechanism that is somewhat different from surface-relief grating structures. With VP gratings, one can achieve higher diffraction efficiencies, higher dispersion for transmissive gratings, and a range of versatility that is not possible with surface-relief gratings. Eventual utilization of this technology into astronomical spectrographs will enhance, complement, and possibly replace the suite of spectroscopic facilities currently in use.

7. ACKNOWLEDGEMENTS

S. Barden wishes to thank S. Wolff for the funds to purchase the test grating and to establish a collaboration with Kaiser Optical Systems, Inc. Appreciation also goes to Di Harmer for her assistance in performing the on-sky testing of the grating. We also give thanks to Dan Schroeder and Richard Elston for their input into early and ongoing discussions regarding the utilization of this technology in astronomy.

8. REFERENCES

1. J. A. Arns, "Holographic Transmission Gratings Improve Spectroscopy and Ultrafast Laser Performances", *Proc. SPIE* **2404**, pp. 174-181, 1995.
2. R. J. Collier, C. B. Burckhardt, and L. H. Lin, *Optical Holography*, Academic Press, New York, 1971.
3. D. H. Close, "Optically Recorded Holographic Optical Elements", *Handbook of Optical Holography*, ed. H. J. Caulfield, Academic Press, New York, 1979.
4. R. Magnusson and T. K. Gaylord, "Analysis of multiwave diffraction by thick gratings", *J. Opt. Soc. Amer.* **67**, pp. 1165-1170, 1977.
5. T. K. Gaylord and M. G. Moharam, "Analysis and applications of optical diffraction by gratings", *Proc. IEEE* **73**, pp. 894-937, 1985.
6. C.B. Burckhardt, "Diffraction of a plane wave at a sinusoidally stratified dielectric grating", *J. Opt. Soc. Am.* **56**, pp. 1502-1509, 1966.
7. R. Magnusson and T.K. Gaylord, "Equivalence of multiwave coupled-theory and modal theory for periodic-media diffraction", *J. Opt. Soc. Am.* **68**, pp. 1777-1779, 1978.

8. H. Kogelnik, “Coupled wave theory for thick hologram gratings”, *The Bell System Technical Journal* **48**, pp. 2909-2947, 1969.
9. E. G. Loewen and E. Popov, *Diffraction Gratings and Applications*, Marcel Dekker, New York, 1997.
10. T. A. Shankoff, “Phase holograms in dichromated gelatin”, *Applied Optics* **7**, pp. 2101-2105, 1968.
11. D. H. Close and A. Graube, “Holographic Lens for Pilot’s Head-up Display”, *NTIS Rep.* **AD/787605**, 1974.
12. B. J. Chang and C. D. Leonard, “Dichromated gelatin for the fabrication of holographic optical elements”, *Applied Optics* **18**, pp. 2407-2417, 1979.
13. R. K. Curran and T. A. Shankoff, “The Mechanism of Hologram Formation in Dichromated Gelatin”, *Applied Optics* **9**, pp. 1651-1657, 1970.
14. D. Corlatan, M. Schafer, and G. Anders, “Wavelength shifting and bandwidth broadening in DCG”, *Proc. SPIE* **1507**, pp. 354-364, 1991.
15. C. Rich and J. Petersen, “Broadband IR Lippmann holograms for solar control applications”, *Proc. SPIE* **1667**, pp. 165-171, 1992.
16. C. de Castro Carranza, A. M. de Frutos Baraja, J. A. Aparicio Calzada, F. A. Frechoso Escudero, S. Caceres Gomez, and J. L. Molpeceres Criado, “Holographic grating with two spatial frequencies for the simultaneous study of two spectral profiles”, *Applied Optics* **31**, pp. 3131-3133, 1992.
17. H. Owen, D. E. Battey, M. J. Pelletier, and J. B. Slater, “New spectroscopic instrument based on volume holographic optical elements”, *Proc. SPIE* **2406**, pp. 260-267, 1995.
18. J. M. Tedesco, H. Owen, D. M. Pallister, and M. D. Morris, “Principles and Spectroscopic Applications of Volume Holographic Optics”, *Analytical Chemistry* **65**, pp. 441A-449A, 1993.
19. S. Vogt et al., “HIRES: The high resolution Echelle spectrometer on the Keck 10-meter telescope”, *Proc. SPIE* **2198**, pp. 362-375, 1994.
20. H. Dekker, “An Immersion Grating for an Astronomical Spectrograph”, *Instrumentation for Ground-Based Optical Astronomy Present and Future*, ed. L. B. Robinson, pp. 183-188, Springer-Verlag, New York, 1988.
21. S. F. Su and T. K. Gaylord, “Calculation of arbitrary-order diffraction efficiencies of thick gratings with arbitrary grating shape”, *J. Opt. Soc. Amer.* **65**, pp. 59-64, 1975.
22. R. Alferness, “Analysis of propagation at the second-order Bragg angle of a thick holographic grating”, *J. Opt. Soc. Amer.* **66**, pp. 353-362, 1976.
23. S. K. Case and R. Alferness, “Index Modulation and Spatial Harmonic Generation in Dichromated Gelatin Films”, *Applied Physics* **10**, pp. 41-51, 1976.
24. R. Vila, A. M. de Frutos, and S. Mar, “Design of aberration-balanced high-efficiency focusing holographic gratings”, *Applied Optics* **27**, pp. 3013-3019, 1988.